



# Treball Final de Grau

**Nanostructured Surface wettability and their interaction with lipid vesicles. A computational analysis of the involved intermolecular forces.**

**Bagnabilitat de superfícies nanoestructurades i la seva interacció amb vesícules lipídiques. Anàlisi computacional de les forces intermoleculars implicades.**

Marcos Carrera Acosta

*June 2023*





Aquesta obra està subjecta a la llicència de:  
Reconeixement–NoComercial–SenseObraDerivada



<http://creativecommons.org/licenses/by-nc-nd/3.0/es/>



Primero de todo, agradecer a Dra. Ilaria Mannelli por su gran implicación y por toda la ayuda que me ha proporcionado en la realización del trabajo.



**REPORT**





## **IDENTIFICATION AND REFLECTION ON THE SUSTAINABLE DEVELOPMENT GOALS (SDG)**

This project focuses on studying the interaction modes of coated self-assembled monolayers with different solvents and lipid vesicles. As cells are enveloped by a cellular membrane, the analysed information can be linked to the behaviour of a specific surface towards the cells, giving useful information about their antiseptic and bactericidal properties. Out of all the areas comprised under the 2030 Agenda, the project can be linked to People and Prosperity areas.

More concretely, regarding the People area's SDGs, this work belongs into SDG 3: good health and well-being, as the different surfaces extensively analysed on this work have been linked with a medical-focused application.

In addition, the project also falls under the Prosperity area, as it aims for goals comprised under SDG 8: decent work and economic growth. One of the goals of the project is to know how the surfaces interact with living cells and their bactericidal properties, objective that comprises target 8.8: safe working environments.



# CONTENTS

<b>1. SUMMARY</b>	3
<b>2. RESUMEN</b>	5
<b>3. INTRODUCTION</b>	7
3.1. Coarse - Grained Modelling	8
3.2. Surface free energy	10
<b>4. OBJECTIVES</b>	12
<b>5. THEORETICAL SECTION</b>	13
5.1. Solvent conformations	13
5.1.1. Contact angle determination	13
5.2. Surface free energy determination	15
5.2.1. OWRK model	15
5.2.2. Wu's model	16
5.3. Solvent election	16
5.4. Computational details	17
5.4.1. Bead types	17
5.4.2. Non-bonded interactions	18
5.4.3. Bonded interactions	19
5.4.4. Chemical polarity	20
<b>6. EXPERIMENTAL SECTION</b>	21
6.1. Substrate – Solvent interactions	21
6.1.1. Contact angle data	21
6.1.2. Interaction energy data	24
6.1.3. Observations	27
6.2. Substrate – Vesicles interaction	28
6.2.1. Interaction energy data	28
6.2.2. Observations	29

---

6.3. Surface free energy determination	29
6.3.1. OWRK model	30
6.3.2. Wu's model	31
6.3.3. Numerical determination	31
6.3.4. Observations	33
6.4. Simulation of new surfaces	33
6.4.1. Interaction with vesicles	34
<b>7. CONCLUSIONS</b>	37
<b>8. REFERENCES AND NOTES</b>	39
<b>9. ACRONYMS</b>	41
<b>APPENDICES</b>	43
Appendix 1: GROMACS input files.	
Appendix 3: Fortran programs – SAM generation	
Appendix 3: Python programs – data analysis	

# 1. SUMMARY

Research on how cells interact with different entities is a main topic in multiple fields of the scientific community, chemistry included. When a cell and a solid interact, the molecular-scale mechanisms of the interaction between the lipidic membrane of a cell and the surface of a solid are poorly understood due to experimental limitations. Computer simulations are used with the objective to surpass these difficulties, so a greater understanding of the mechanisms can be gained. More precisely, coarse-grained molecular dynamics simulations are the elected tools when studying these processes, involving lipid vesicles, at the molecular level. In this project, simulations have been conducted to study the interactions between solvents and lipid vesicles with a wide variety of contacting surfaces whose physicochemical properties are adjusted by coating them with different series of neutral molecules and varying their heights.

The motivation of the simulations is to firstly, obtain information of the surface free energy of the solid, a property related to wetting, and then perform an exhaustive analysis of the nature of the surface and the molecular-scale mechanisms of its interaction with the lipidic vesicle. The software package chosen to perform the simulations has been GROMACS (Groningen Machine for Chemical Simulations). Furthermore, the data derived from the simulations has been analyzed with a Python script.

**Keywords:** Lipidic vesicles, contacting surfaces, surface free energy, wettability, molecular dynamics simulations.



## 2. RESUMEN

Los estudios de la interacción de las células con diferentes entidades es uno de los principales tópicos en diferentes campos de la comunidad científica, incluida la química. Cuando una célula y un sólido interactúan, los mecanismos que se producen en la escala molecular entre la membrana lipídica de la célula y la superficie del sólido no son plenamente entendidos, principalmente por limitaciones experimentales. Las simulaciones computacionales se emplean para superar estas dificultades, ganando conocimiento sobre los mecanismos previamente mencionados. Más precisamente, las simulaciones de dinámica molecular de grano grueso son las escogidas para estudiar este tipo de procesos, que implican vesículas lipídicas, a escala molecular. En este proyecto, las simulaciones se han realizado para estudiar las interacciones entre solventes y vesículas lipídicas con una amplia variedad de superficies de contacto, cuyas propiedades fisicoquímicas han sido ajustadas con una serie de moléculas neutras y variando sus alturas.

La motivación de las simulaciones es, primeramente, obtener información de la energía libre superficial de sólido, propiedad relacionada con el mojado. Una vez hecho, se realiza un análisis exhaustivo de la naturaleza de la superficie y de los mecanismos a escala molecular de su interacción con la vesícula lipídica. Para ello, el software de GROMACS (Groningen Machine for Chemical Simulations) ha sido escogido. Adicionalmente, los datos derivados de las simulaciones han sido analizados mediante un script de Python.

**Palabras clave:** Vesículas lipídicas, superficies de contacto, energía libre superficial, mojado, simulaciones de dinámica molecular.





### 3. INTRODUCTION

The area that studies materials, materials science is an interdisciplinary branch of science, mainly based on chemistry and physics phenomena, focused on researching how the structure affects a material at several scales, such as electronic, micro and macroscale. Materials science is also responsible for investigations aiming for discovering new materials and determining its properties and performance on certain tasks. [1]

The world has experienced an important evolution in the computational field over the last decades, and the field of materials science has been no exception, as it has seen an enormous growth in computational power availability. This has affected the work of many scientists in the area, generating the ability to solve complex problems thanks to the use of the computational tools, even to the point that nowadays they are indispensable in the world of materials research and development. Parallel to this growth, advancements in various methods, such as mathematics or materials theory, have provided the foundation on which these new computational tools are based. [2]

Contextualizing with the contents of the project, simulating the behaviour of natural systems using computational methods has become possible to a large degree, as the simulated data is becoming less erroneous and more in line with the data from actual experiments. On this case, the properties of surfaces have been modified, so their interaction with lipidic membranes can be monitored. On top of that, the amount of data generated via computational simulations is large, as computers solve complex mathematical models aiming for a certain numerical solution. The simulation of experiments with certain computational tools and a subsequent data analysis has become the norm in the research that is done today, since without it valid conclusions could not be drawn.

On the other hand, one of the main problems in any scientific project linked to biology is the difference in both temporal and spatial scales between the experimental observation and the computational simulation of a biological system.

Chemical reactions and processes, the main basis of the phenomena taking place in living beings, is the main point that is observed in a non-invasive way to provide a better understanding of life, however, these experimental techniques present a great limitation caused by their time scale, since it is very difficult to observe at times greater than the microseconds. However, there are theoretical methods that allow the formation of computational models to study a system, such as molecular modelling, which allows to describe a real system with all levels of detail. Currently, computational methods have great limitations, as an example, a simulated system must be small, approximately up to 10 nm or even smaller if the simulation is conducted on a large temporal scale. In addition, the time limitation is also present during computational simulations, as an expansion in the temporal scale also consumes computational resources. It should be noted that other computational models allow the system to be expanded, like coarse-grained modelling, trying to achieve the size that is observed during experimental techniques, with a time scale in the order of microseconds.<sup>[3]</sup>

In this study, coarse-grained modelling techniques are applied to obtain information about a critical point in materials science: the wetting properties of a surface. Wettability is a property of a surface that directly indicates its surface free energy, a property being related to especially important phenomena such as the biological response to a material.<sup>[4]</sup>

To conduct the technique, nanostructured surfaces are constructed and coated with neutral particles whose properties of hydrophobicity, oleophobicity and polarity can be determined. For this, the system is constructed with molecules that can make a self-assembled monolayer. The constructed surfaces are differentiated in the number of nanopillars per area. Specifically, arrays of 3x3, 4x4, 6x6 and 8x8 nanopillars are constructed, each one with heights of 2, 5 and 10 nm. Once the surfaces are done, the interaction energies and contact angle with a solvent and the interaction energy with a lipid vesicle are studied, in this way, its surface free energy and its mode of interaction with lipidic elements can be estimated.

### **3.1. COARSE-GRAINED MODELLING**

To carry out the coarse-grained modelling of our system, we will work with GROMACS software, a molecular dynamics package specially designed to carry out simulations of systems with proteins, lipids, nucleic acids, systems that usually are conformed by a high number of atoms. To perform the simulations, the MARTINI force field will be used.

The main characteristic of the MARTINI force field is the 4:1 mapping employed, where every four heavy atoms a coarse-grained interaction point is made. Each interaction point, also called a bead, belongs to a certain category based on its main characteristics. In the attached table, the compilation of all the beads and an example of each type is attached. [5]

Bead type	Q <sub>da</sub>	Q <sub>d</sub>	Q <sub>a</sub>	Q <sub>0</sub>	P <sub>5</sub>	P <sub>4</sub>	P <sub>3</sub>	P <sub>2</sub>	P <sub>1</sub>
Example	H <sub>3</sub> N <sup>+</sup> - C <sub>2</sub> - OH	H <sub>3</sub> N <sup>+</sup> - C <sub>3</sub>	Na <sup>+</sup> OH <sup>-</sup>	PO <sub>4</sub> <sup>-</sup>	H <sub>2</sub> N- C <sub>2</sub> =O	HOH (x4)	HO- C <sub>2</sub> - OH	C <sub>2</sub> - OH	C <sub>3</sub> - OH
Bead type	N <sub>da</sub>	N <sub>d</sub>	N <sub>a</sub>	N <sub>0</sub>	C <sub>5</sub>	C <sub>4</sub>	C <sub>3</sub>	C <sub>2</sub>	C <sub>1</sub>
Example	C <sub>4</sub> - OH	H <sub>2</sub> N- C <sub>3</sub>	C <sub>3</sub> =O	C-O- C <sub>2</sub>	C <sub>3</sub> - SH	C-X <sub>4</sub>	C <sub>3</sub> -X	C <sub>3</sub> H <sub>8</sub>	C <sub>4</sub> H <sub>10</sub>

Table 1: Basic bead types and an example of multiple molecules that can be modelled with them on MARTINI force field. Type Q beads fulfil the function of a charged interaction centre. Type P beads indicate a polar interaction centre. Type N beads correspond to non-polar beads. Finally, type C beads are totally apolar beads. The subscript indicates the behaviour: d= donor, a= acceptor, da= both, 0= nothing. Also a numerical notation is used on P and C beads, where 5 are the most polar and 1 the least.

In the project, the modelling of a molecule in the all-atom style to a coarse-grained one has been conducted. To do this, there are several rules to keep in mind, with the goal of reproducing the thermodynamic properties of the original molecule: [5]

- Only the heavy atoms (other than hydrogen) are the ones that define the mapping of the molecule.
- In the case that a molecule possesses a functional group, this cannot be divided between different points of interaction.
- The symmetry of the molecule must be respected: the priority is to respect the shape of the all-atom model.
- 4:1 regular (R), 3:1 small (S) or 2:1 tiny (T) mappings are possible, where R-type beads are the best in terms of computational performance.

Detailing about how the force field is created, the peculiarity of the Martini force field is that it has several contributions that are optimized by comparing the simulated results with experimental data. Such contributions are the bonds, angular, improper dihedrals, torsions, electrostatics, and Van der Waals contributions, generating the following equation:

$$U = \sum \left(\frac{1}{2}\right) K_b (b - b_0)^2 + \sum \left(\frac{1}{2}\right) K_b (\theta - \theta_0)^2 + \sum K_\phi [1 - \cos(n\phi)]^2 + \sum \varepsilon_{ij} \left[ \left(\frac{R_{ij}}{r_{ij}}\right)^{12} - 2 \left(\frac{R_{ij}}{r_{ij}}\right)^6 \right] + \sum \frac{q_i q_j}{4\pi \varepsilon_0 \varepsilon r_{ij}} \quad (1)$$

Previously to the development of MARTINI force field, coarse grained models were used in a wide variety of simulation techniques, as it was proven to be a valuable tool to study systems beyond what is possible with all-atom models, due to it being a simplified version. A large variety of force fields were available to apply to coarse grained techniques, such as qualitative methods, solvent-free methods, etc. MARTINI force field was originally created with the objective to be a suitable force field for a wide variety of applications, without the need to reparametrize any variable each time. To achieve that feature, the data of the different building blocks was calibrated against experimental thermodynamic data.

### 3.2. SURFACE FREE ENERGY

In the study of the wetting properties of a solid, the surface free energy, from now on abbreviated as SFE, is one of the key parameters. It is equivalent to the surface tension of a solid. The SFE describes the work necessary to increase the surface area of a solid phase, therefore, it is an important parameter for the optimization of liquid-solid contact processes. It is indicated as free energy since it is the part of the energy that can be converted into mechanical work, in contrast to internal energy that contains terms related to entropy. To relate the SFE with the wettability of a surface, we must consider that all systems tend to evolve to their most stable state, that is, their lowest energy state. To do this, liquids contact the smallest possible area due to surface tension. On the contrary, solids cannot minimize the surface by deformation, but they can form an interface to decrease the SFE as much as possible. This interface is the wetting region when liquids contact solids. A good wettability of the solid corresponds to high SFE, while lower values are related to applications such as protection against corrosion and humidity, where the interaction between the liquid and the surface is avoided.

To obtain information about the wetting properties of the nanostructured surfaces it is necessary to know the contact angle of the solvents with the different nanopillars in the first

instance. This will allow to determine the surface free energy, which together with the determination of the polar and disperse parts of the SFE, will enable us to perform the wetting profile of the surface. This topic is further explained on theoretical section.

Before concluding the introduction, is important to note that SFE originates from molecular interactions at the surface. The attached figure represents a solid:

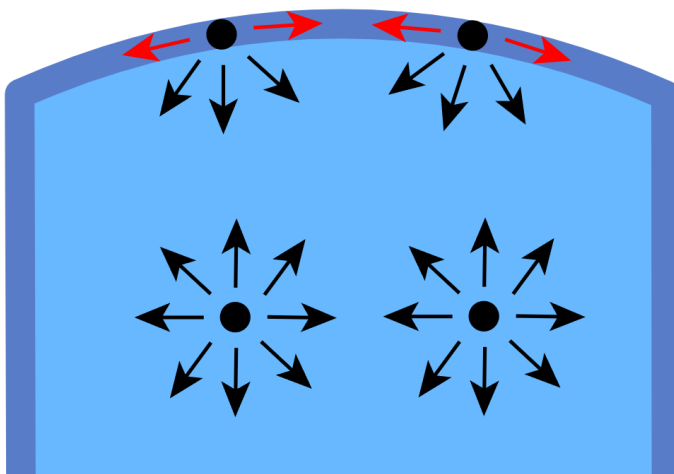


Figure 1. Surface free energy, superficial molecules don't present attractive forces to a top layer. (Created by user Booyabazooka, 17/05/23 via Wikimedia Commons, Public domain)

The atoms present at the surface don't match the number of neighbouring atoms compared to interior atoms, as there is not a layer on top of them. This fact generates an excess force at the surface, which is dependent on the strength of the interactions between the atoms in the solid. On solids whose bonds are strong, such as metal bonds on a metallic body, the SFE acquires high values, whereas polymeric substances that contain weak bounds originate a low SFE value. Thermodynamically, high SFE values can be linked to unstable systems, so, the material will need to stabilize the system. To achieve that, metals grow oxidized layers on top of them, creating a state with a lower surface free energy. On the other hand, polymers with lower SFE values are more suitable to not suffer any change.

## 4. OBJECTIVES

The objective of this work is to analyse the interaction of the solvents with the contacting surfaces to determine their SFE and characterize the wetting properties of the surfaces. Apart from that, the action of the nanostructured surfaces on lipid vesicles is studied in terms of the interaction energy and the molecular mechanisms that both undergo during the interaction. To fulfil the objective, firstly, the surface free energy will be determined by contact angle data of a solvent on a specific surface. The interaction energy between solvent and surface will provide information on the nature of the latter. Then, in a simulation system with the surface and the lipidic vesicle, information on both the molecular mechanisms of vesicle conformation changes and their associated energy balances will be obtained, so it will be linked directly with the suitable applications for the surface. The work will be conducted using the GROMACS software, in which it is possible to simulate different coarse-grained systems and analyse their evolution.

## 5. THEORETICAL SECTION

### 5.1 SOLVENT CONFORMATIONS

Solvent droplets can be found in different conformations on the nanostructured surface, either the Cassie-Baxter state or the Wenzel state.

The Cassie-Baxter state is characteristic of solvents left in contact with the peaks of the pillars with air trapped between the surface apertures, making the solvent to not be in complete contact with the surface. On the other hand, in Wenzel state the solvents are fully contacting the surface, generating a higher degree of interaction between both parts thus resulting in a higher degree of contact between the systems. Although the previously mentioned differences, both states are relatively stable and the main characteristics that modulate a surface so that one state is the dominant are the size of the pillars, the spacing between them and the intrinsic contact angle, apart from the stability of the interaction between both parts. [6,7] In the cases studied, the size of the pillars is the factor that causes the observable differences.

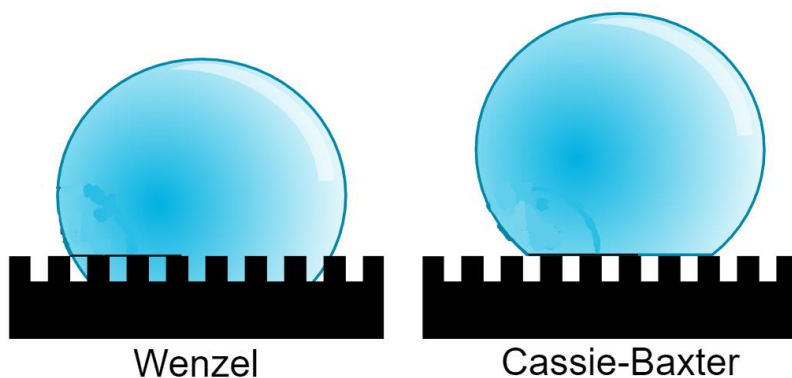


Figure 2. Cassie and Wenzel wetting states. Wenzel state, represented on the left, has lower energy compared to Cassie-Baxter, which is a meta-stable state. [8] (Created by user Vladsinger, 29/04/23 via Wikimedia Commons, Creative commons 3.0, the text inside the droplet has been erased).

#### 5.1.1. Contact angle determination.

When an interface is created between a liquid and a solid, the angle between the surface of the liquid and the surface with which it is in contact is described as the contact angle ( $\theta$ ).

The contact angle will have different values depending on how good the wetting is. In the case of complete wetting, the liquid will be fully extended in the solid, with  $\theta=0^\circ$ . Between  $0^\circ$  and  $90^\circ$ , the solid is being wet and any value above  $\theta=90^\circ$  indicates the opposite. In the case of surfaces that do not allow these interactions lotus effect is found, where values are close to  $\theta=180^\circ$ . [9]

It is important to note that considering the equilibrium of forces in the wetting of a solid, it is possible to relate the measure of the contact angle with the surface free energy by means of Young's equation [10], the following schematic of the forces acting on a droplet illustrates this:

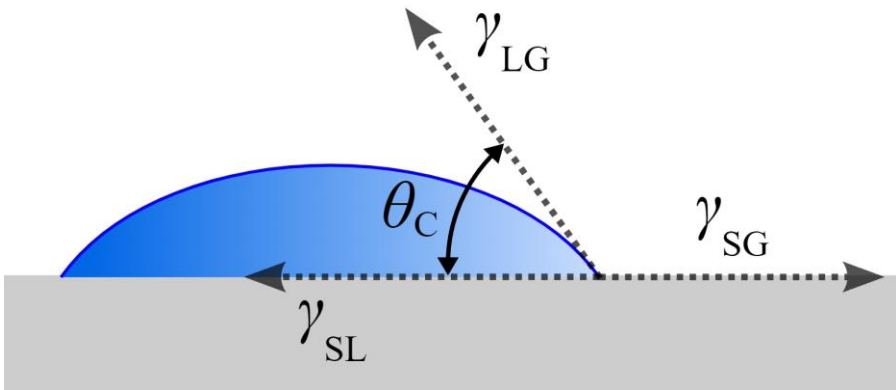


Figure 3. Main forces acting on a droplet – solid system and schematization of the contact angle.  $\gamma_{LG}$  will be referenced from now on as  $\sigma_l$  and  $\gamma_{SL}$  as  $\sigma_s$ , the meaning of the different parameters is listed below. (Created by user Joris Gillis~commonswiki, 29/04/23 via Wikimedia Commons, Public domain)

$$\sigma_s = \sigma_{ls} + \sigma_l \cdot \cos \theta \quad (2)$$

- $\sigma_s$  is surface free energy of the solid
- $\sigma_l$  is surface tension of the liquid
- $\sigma_{ls}$  is the tension at the interface
- $\theta$  is the contact angle

Another key data that must be collected apart from contact angle is the interaction energy between both parts of the simulated system. The energy derived from the interaction between the solvent and the different beads of the surface indicates the nature of the surface. As an example, high interaction energies between the surface and an apolar liquid, such as hexadecane, are



indicatives of oleophobicity of the surface. So, if a surface is contacted by different solvents whose polarities are differentiated and their interaction energies are calculated, the nature of the surface can be classified.

## 5.2 SURFACE FREE ENERGY DETERMINATION

As mentioned under the previous section, Young's equation defines us the mathematical expression of the surface free energy:

$$\sigma_s = \sigma_{ls} + \sigma_l \cdot \cos \theta \quad (2)$$

Where the parameter  $\sigma_{ls}$ , relative to the tension at the interface, can be obtained from the following expression:  $\sigma_{ls} = \sigma_l + \sigma_s - (\text{Interactions between the two phases})$ . (3)

It should be noted that there are multiple methods to calculate the interactions between the two phases. The most typical subdivision that is usually used is to divide the interactions between polar and disperse types, making the same division for surface free energy calculations.

To determine the surface free energy, the contact angles must be measured with at least two different liquids whose surface tensions and polar and disperse fractions are known. Finally, Young's equation is combined with the equation 3 so it is possible to incorporate these interactions, allowing the calculation of  $\sigma_s$ .

### 5.2.1. OWRK model

A useful approximation is the Owens-Wendt-Rabel-Kaelble model, which builds up on Fowkes method, dividing interfacial tension:  $\sigma_{ls}$  into  $\sigma_s$  and  $\sigma_l$  and the geometric mean of the interactions between their coincident components. It notes that any parameter indicative of the surface tension can be divided into a dispersive component -  $\sigma^D$ , which takes in account forces like, as an example, London dispersion forces, and a polar component -  $\sigma^P$ , indicative of polar forces, such as hydrogen bonding. Equivalently,  $\sigma_s$  is also the sum of a polar and a disperse part. In this method, the expression resulting from Young's equation with the determination of the interactions between the phases is:

$$\sigma_{ls} = \sigma_l + \sigma_s - 2 (\sqrt{\sigma_s^D \sigma_l^D} + \sqrt{\sigma_s^P \sigma_l^P}) \quad (4)$$

As said under section 5.2, at least two liquids with known polar and disperse parts of surface tension are necessary. One of them must have a positive polar part. Therefore, solvents such as

water can be used while the other one must be completely dispersive, like hexadecane or diiodomethane.<sup>[11]</sup> The solvents used in this project will be discussed in a future section. According to the method, the value of interfacial tension depends on the possibility of polar and disperse parts to form interactions with the matching parts of the complementary phase.

### 5.2.2. Wu's model

One of the main methods for the calculation of the SFE is the Wu model, mostly applied in polymers with a low surface energy (approx. 40 mN/m).

In this method, the variable  $\sigma_{ls}$  is calculated as the sum of the surface tensions of the liquid and the solid together with the harmonic mean of the surface tensions in the dispersed and polar part, obtaining the expression:

$$\sigma_{ls} = \sigma_l + \sigma_s - 4 \left( \frac{\sigma_s^D \sigma_l^D}{\sigma_s^D + \sigma_l^D} + \frac{\sigma_s^P \sigma_l^P}{\sigma_s^P + \sigma_l^P} \right) \quad (5)$$

## 5.3 SOLVENT ELECTION

As indicated previously, in the determination of the SFE there are different unknown variables, referred the polar and dispersed part of  $\sigma_s$  if Wu or OWRK model is applied.

If two solvents are selected, one of the liquids must be polar, while the other must be completely dispersive. Water is the most common polar liquid, although it is also common to perform the determination with glycerol. While the most common completely dispersive liquids are hexadecane and diiodomethane since they have high surface tension values even though their completely dispersive nature. Three solvents can also be used to solve the problem, forming a third equation on the mathematical system.

In the case of using three liquids in the determination of the SFE, the third is typically a polar liquid, such as glycerol, or benzyl alcohol to prevent the high polar contribution of water from being a cause of error in the calculation of the SFE due to strong hydrogen bonding.<sup>[12,13]</sup> The following table shows the properties of the solvents mentioned in previous sections.

High surface tensions cause the contact angle to be measurable on most surfaces, so it is also a priority.

	$\sigma_i$ [mJ/m <sup>2</sup> ]	$\sigma_i^D$ [mJ/m <sup>2</sup> ]	$\sigma_i^P$ [mJ/m <sup>2</sup> ]
Water [14]	72.8	21.8	51.0
Diiodomethane [15]	50.8	50.8	0
Hexadecane [14]	27.6	27.6	0
Benzyl alcohol [16]	39.0	30.3	8.7
Glycerol [15]	64.0	36.3	27.7
Ethanol [15]	23.2	21.2	2.0

Table.2: Compilation of polar and dispersive components of typical solvents used during SFE determination measurements. Values are given in  $J \cdot 10^{-3}$  per unit of area, equivalent to mN/m. In this project, water, hexadecane, and ethanol are selected.

## 5.4 COMPUTATIONAL DETAILS

To perform the simulations, different software packages are used. Molecular dynamics simulations of the system are conducted with the md integrator built in GROMACS. Md integrator is a leap-frog algorithm that integrates Newton's equations of motion:

$$p = mv; F = ma; F_{1 \rightarrow 2} = -F_{2 \rightarrow 1},$$

And applies the equations to every particle in the system, on this case conformed of neutral molecules part of the surface, such as sup, supf and dec and the solvent, so the different forces that every particle undergoes can be calculated.

### 5.4.1. Bead types

To perform a suitable model of a surface, various types of beads are generated. The following table contains a summary of the different beads that must be generated:

System part	Bead name	Bead type	Description
Surface	SUP	NaN	Neutral particle
Surface (Antifreeze)	SUPF	NaF	Bigger neutral particle
Coating	DEC	C <sub>1</sub>	Alkane particle
Coating type 2	D2F	CX	Bigger alkane particle

Table.3: New bead types introduced to model the DEC surface.

Surface molecules are represented by SUP beads, consisting of neutral particles that interact in a semi-repulsive form with apolar particles and in a semi-attractively with charged particles. SUPF beads, generated to achieve better computational results and prevent the possible freezing of the surface caused by self-interaction are essentially a version of SUP beads with a higher radius to modify the lattice packing, and higher repulsion for polar beads so the antifreeze function is accomplished. On the simulations, up to 15% of the normal particles are being replaced by antifreeze particles to achieve the desired effect.

In addition to that, surfaces are usually coated with modifiers, on this project, they are coated with dodecane, a neutral hydrocarbon represented with 3 apolar beads on coarse-grained simulations, one of which is anchored to the surface or D2F, its fluorinated version on the “tail” beads.

Solvents are modelled following the same logic. Apolar solvents, such as hexadecane, are just represented with a single bead type. However, polar solvents suitable to self-interact, must be divided in a normal bead and an antifreeze bead, so the solvent is free to move around during the simulation.

#### 5.4.2. Non-bonded interactions

The Lennard-Jones potential is referred to an intermolecular pair of potential interactions. It models soft repulsive and attractive interactions comprised under the van der Waals category of interactions, so it can describe electronically neutral atoms and molecules. Lennard-Jones perfectly fits under this project, due to both the solvent and the surface consisting of a series of

neutral molecules. The expression for the Lennard-Jones potential is also included under the MARTINI force field, as:

$$V_{LJ}(r) = 4\varepsilon\left[\left(\frac{\sigma}{r}\right)^{12} - \left(\frac{\sigma}{r}\right)^6\right] \quad (6)$$

- $r$  is the distance between the interacting particles
- $\varepsilon$  is the dispersion energy
- $\sigma$  is the distance where the potential energy achieves zero

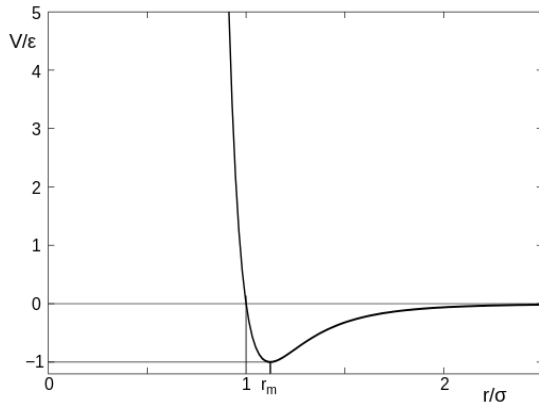


Figure 4. Representation of the Lennard-Jones potential. X-axis denotes a function of the distance between molecules, while Y-axis is the intermolecular potential energy. (Created by user Olaf Lenz and Rainald62, 30/04/23 via Wikimedia Commons, GNU Free Documentation License)

The potential model describes the basic features of interactions between atoms and molecules: molecules do not interact at infinite distance, they attract each other at moderate distances and repel each other at close distances.

### 5.4.3. Bonded interactions

Bonded interactions between beads of the same molecule are described by a weak harmonic potential under MARTINI force field as:

$$V_{bond}(R) = \frac{1}{2}K_{bond}(R - R_{bond})^2 \quad (7)$$

Bonded particles, on average closer to each other than nonbonded particles, only use a single equilibrium bond distance and a force constant to define the potential. This expression doesn't consider Lennard-Jones type interactions.

#### 5.4.4. Chemical polarity

It is important to define chemical polarity, as it is one of the main properties that can be quickly calculated and simulated for the researcher's interest. Polarity is the measure of electric charge separation, leading a molecule to have an electric dipole moment, with part of it positively charged and another part negatively charged. Polar molecules are generated on a difference in electronegativity between to different bonded atoms, which generates a certain bond dipole. It is important to note that bond dipoles must not cancel each other by means of symmetry to retain its polarity.

On the context of the project, a group of electronically neutral molecules with diverse polarity are generated. To have a better understanding of the interaction energies between the different groups of the system, polarity is the first variable to consider, as polar molecules interact with each other via intermolecular forces such as dipole-dipole interactions, a term that is included in the Lennard-Jones potential.

Derived from polarity, hydrophobicity and hydrophilicity describe how a molecule interact with water. Hydrophilic molecules are those molecules whose interactions with polar substances, such as water, are thermodynamically favourable, so they can be solvated in a polar medium. On the other hand, hydrophobic molecules usually have more favourable interactions with oily solvents, whose characteristic feature is low to zero polarity.

## 6. EXPERIMENTAL SECTION

To achieve our goals, two different types of simulations have been conducted. The first group of simulations are based on a system of the different nanostructured surfaces and a droplet of the solvent. More precisely, the surfaces are formed by an array of 3x3, 4x4, 6x6 or 8x8 nanopillars, ordered in ascending nanopillar per area, with a height of 2, 5 and 10 nm. Additionally, they are coated with DEC beads. This will provide information on the interaction mode between the two entities, generating information about the contact angle and the interaction energy, then helping in the characterization of the nature of the given system and its SFE. The second type of simulation consists of the same surfaces as before and a lipid vesicle, as this will provide information about how the surface may interact with living cells.

### 6.1 SUBSTRATE – SOLVENT INTERACTIONS

#### 6.1.1. Contact angle data.

The analysis of the contact angle is an important part of the project, as it allows to know one of the unknown variables of Young's equation, gaining information on the free energy of the surface. To visualize the contact angle, the system is analysed using VMD. A representation where the solvent and the SAM are clearly differentiated is created. The pictures below show some examples, where the solvent conformation on Cassie-Baxter state and Wenzel state are visible. The first one is Wenzel state, on a surface with 8x8 2nm nanopillars, in contact with water. The other one attached is Cassie-Baxter state on a surface with 6x6 10nm nanopillars also contacting water:

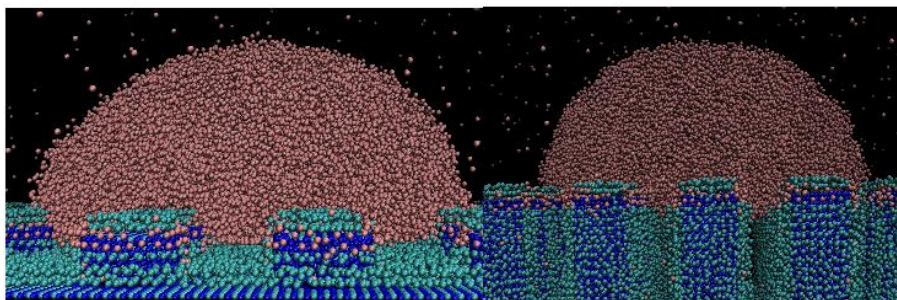


Figure 5: Left side: Wenzel state of a water droplet, where the solvent is extended on the central pillar, creating a higher contact area between the parts. Surface beads are blue and green,

water is shown as red beads. Visualised via VMD. Right side: Cassie-Baxter state of a water droplet. Water can be seen on top of the nanopillars, without intrusion to the surface. Surface beads are blue and green, water is shown as red beads. Notice the intrusion of water on Wenzel state.

The following one is Wenzel state, on a surface with 6x6 5nm nanopillars, contacting hexadecane:

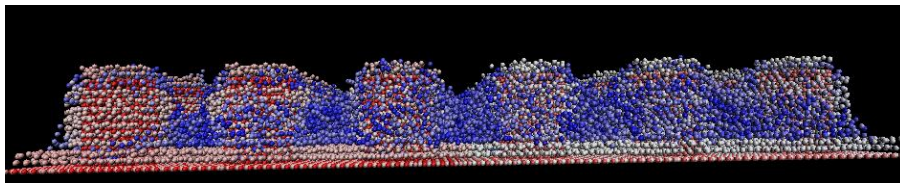


Figure 6: Total wetting of a 6x6 surface with  $h=5$  nm nanopillars with hexadecane. Surface beads are red, white, and light pink, the solvent is shown as blue beads.

A representation of each system is generated like the ones showed before, the contact angles between the solvent – surface and the solvent conformation are determined, the lines to calculate the contact angle are the interface between the solvent and the top of the nanopillar and the tangent to the droplet, neglecting groove volume. The following table provides the collected information.

Nanopillar height	6x6 systems [°]			8x8 systems [°]		
	Water	Hexadecane	Ethanol	Water	Hexadecane	Ethanol
$h= 2$ nm	68 (CB*)	25 (W)	36 (W)	51 (CB*)	22 (W)	<10 (W)
$h= 5$ nm	70 (W)	<10 (W)	<10 (W)	66 (CB*)	<10 (W)	<10 (W)
$h= 10$ nm	73 (CB*)	<10 (W)	<10 (W)	74 (CB*)	<10 (W)	<10 (W)

Table.4: Contact angle data extracted from the simulated systems, the information on parenthesis indicates the state that presents the solvent, CB refers to Cassie-Baxter while W to



Wenzel. Systems marked by CB\* refer to mixed states, where the solvent is found on Cassie-Baxter conformation with a minimal intrusion in the surface. The simulation is an equilibrium of the system divided into  $10 \cdot 10^6$  steps, with a reference temperature of 310 K.

The affinity of the surface for the solvent can be identified. When the solvent fully unfolds, it provokes low contact angles, meaning that the interaction is relatively stable, and the surface has affinity for the type of molecules that are contacting. In these cases, as it is difficult to make a visual estimate of the contact angle of the system, it is indicated that it is  $<10^\circ$ .

On the case of hexadecane, the contact angle is close to  $0^\circ$ , this extraordinary wetting indicates a high value of the affinity of the surface for dispersive molecules thereby a high value of  $\sigma_s^D$  is expected. On the other hand, water is seen on high contact angles, indicative of a contrary tendency of affinity and lower values of  $\sigma_s^P$ .<sup>[17]</sup>

Additionally, the contact angle is also measured between the line where the base of the solvent is found and the tangent to the droplet, so the methodology considers if the solvent enters the nanostructure. With the new calculation method, the following results are obtained:

	6x6 systems [°]			8x8 systems [°]		
Nanopillar height	Water	Hexadecane	Ethanol	Water	Hexadecane	Ethanol
h= 2 nm	110 (CB)	25 (W)	36 (W)	114 (CB)	22 (W)	<10 (W)
h= 5 nm	118 (W)	<10 (W)	<10 (W)	118 (CB)	<10 (W)	<10 (W)
h= 10 nm	122 (CB)	<10 (W)	<10 (W)	124 (CB)	<10 (W)	<10 (W)

Table.5: It is seen how some water systems present way higher contact angle, since water has entered the structure and it must be considered for contact angle calculation following the new calculation method. The table presents the same nomenclature as Table.4.

These values are similar to experimental data present on reference<sup>[18]</sup>, which notes that SAMs coated with a  $C_{18}$  molecule – which differs but is similar to DEC –  $C_{12}$ , present a  $0^\circ$  contact angle for hexadecane and a  $120^\circ$  for water following this contact angle determination method. For the

simplification of the project, further sections have only been calculated with data from Table.4, as it was the first set of contact angles calculated.

### 6.1.2. Interaction energy data

The interaction energy between nanostructured surfaces and solvents has been studied to characterize the nature and wetting properties of the surfaces. It should be noted that, as higher the nanopillar that is created, a surface with more area is generated so the contact between both parts of the system will be incremented. This will expose the energy trends of each surface, so the determination of their nature will be direct. As an example, if the energy of a system becomes less negative when a higher nanopillar is present, it is indicative of a low affinity between both parties, e.g., hydrophobicity or oleophobicity.

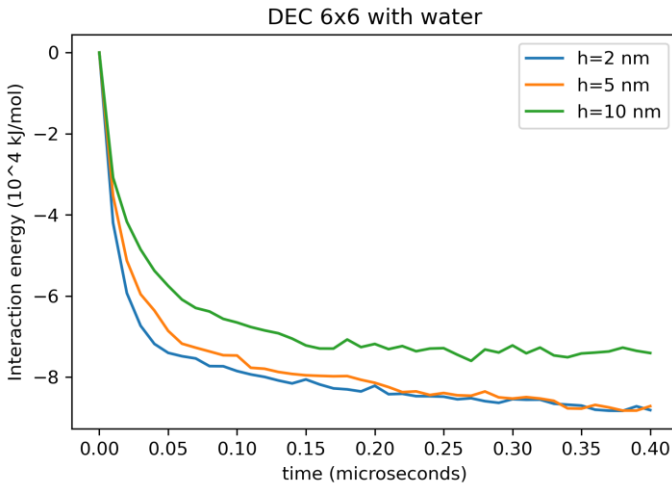


Figure 7: Evolution of interaction energy between water and a 6x6 system with DEC coating. A similar tendency is found on every surface, as they strive to achieve a lower energy as time passes.

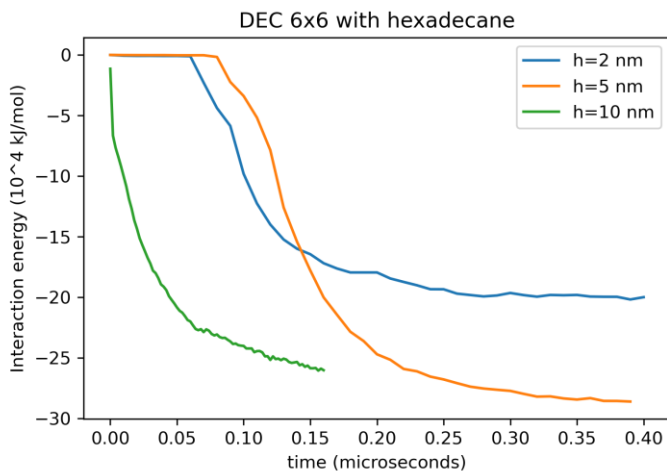


Figure 8: Evolution of interaction energy between hexadecane and a 6x6 system with DEC coating. A trend like that of the previous system is observed, noticing the lower values of energy on this case.

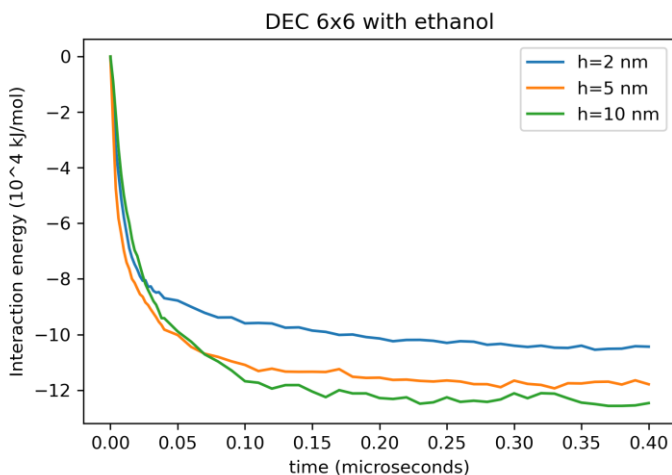


Figure 9: Evolution of interaction energy between ethanol and a 6x6 system with DEC coating. A trend like that of the previous system is observed, it is important to note that energy values are an intermediate step between the previous systems.

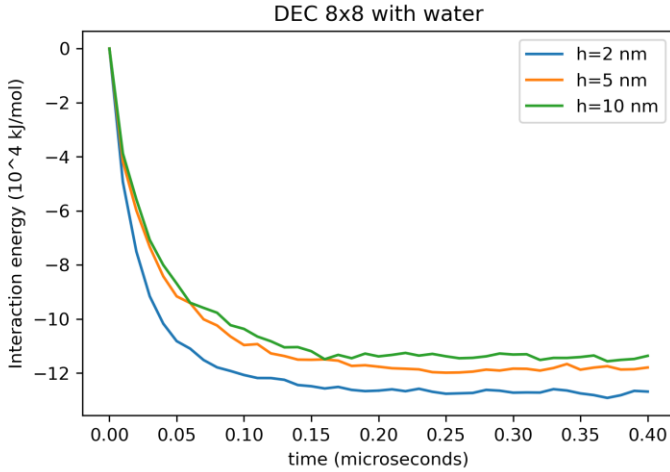


Figure 10: Evolution of interaction energy between water and an 8x8 system with DEC coating. Every water system presents the same pattern, as the higher the nanopillar, the most destabilised the system is.

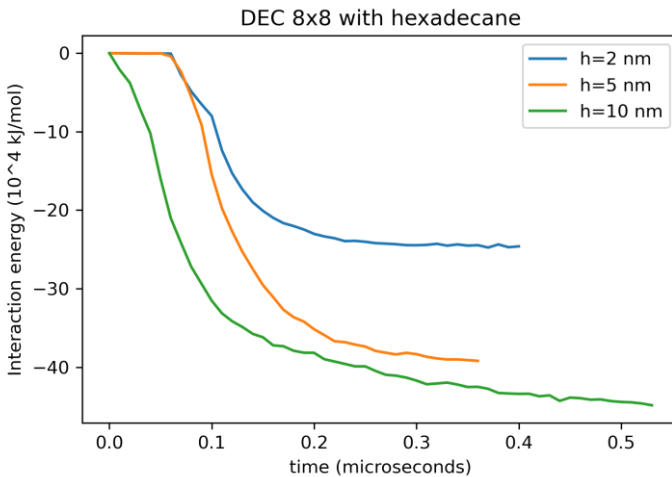


Figure 11: Evolution of interaction energy between hexadecane and a 8x8 system with DEC coating.

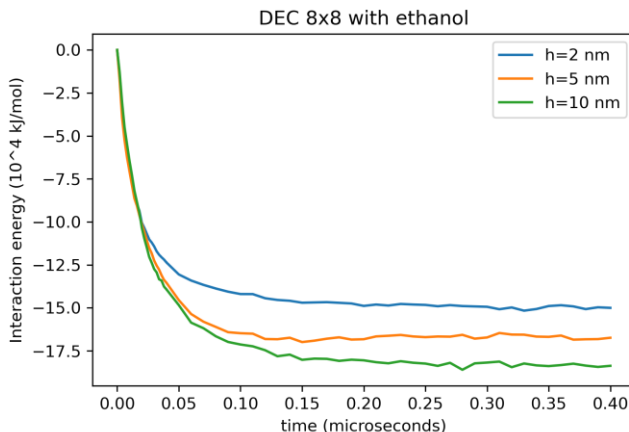


Figure 12: Evolution of interaction energy between ethanol and an 8x8 system with DEC coating. A trend like that of the previous system is observed, it is important to note that energy values are an intermediate step between the previous systems.

### 6.1.3. Observations

On systems whose solvent is water, the energy is less negative compared to other solvents. It can be also seen that the higher the nanopillar, the less stable the system, but still maintaining negative energy values. This trend is caused due to the hydrophobic characteristics of the DEC coating, generating fewer stable systems the greater the contact between water and the surface.

On the other hand, hexadecane solvated systems achieve a lower, more stable, energy with the rising height of the nanopillar. This phenomenon is caused by the interactions that take place between the systems as the coating is oleophilic, so it experiments stable interactions with hexadecane.

Another observation can be drawn from the data: the greater the number of nanopillars, the lower the overall energy, as molecules can interact with each other more easily, allowing for stabler conformations. To obtain the results, the interaction between the solvent, modelled as HD in case of hexadecane, W and WF in case of water or ETOH and ETOHF for ethanol, with the surface, conformed of SUP, SUPF and DEC beads has been studied. Out of all the interactions, those that don't involve antifreeze beads, like SUPF and WF, are the ones that contribute the most to the result, due to the higher abundance of normal beads, indicated in theoretical section as an 85 to 15 ratio.

## 6.2 SUBSTRATE – VESICLES INTERACTIONS

Surface wettability is a property related to especially important phenomena, like the biological response to a material, as mentioned previously and stated on reference [4]. So, it is directly linked to the ability of cells to interact with different surfaces. Basic simulations have been conducted, consisting of simple lipid vesicles interacting with 3x3 and 4x4 nanopillars surfaces with varying nanopillar height, aiming for knowledge on the fundamental interaction mechanisms taking place between the surfaces. The reason of including lipid vesicles on the simulation system is that they are used to emulate a biological envelope, such as cellular membranes, complex systems composed of a mix of lipid and protein molecules, so the interface between a given surface and a living organism would be simulated. To create a system like that, a vesicle made of cholesterol and POPC, a lipid used to simulate lipid rafts, is generated. It is important to notice that lipid vesicles don't interact following the same mechanism with surfaces whose coating properties differ, so the interaction energy data can't be extrapolated if a different type of coating, other than DEC is used.

### 6.2.1. Interaction energy data.

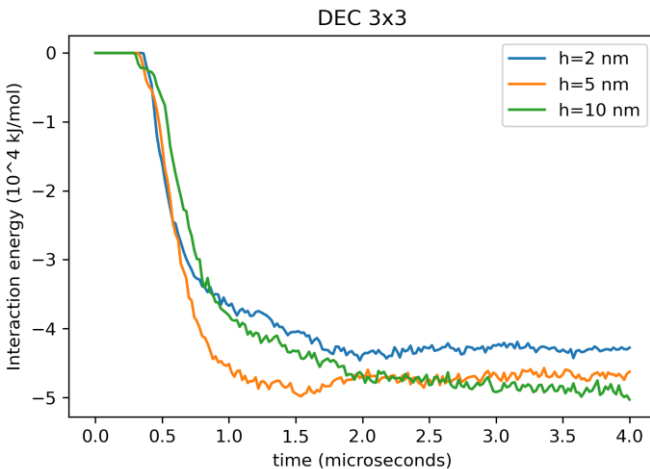


Figure 13: Evolution of interaction energy between a lipidic vesicle and a 3x3 SAM system with DEC coating. The modelled vesicle interacts with DEC coating, as it is oleophilic, so a stable system is formed as the simulation proceeds.

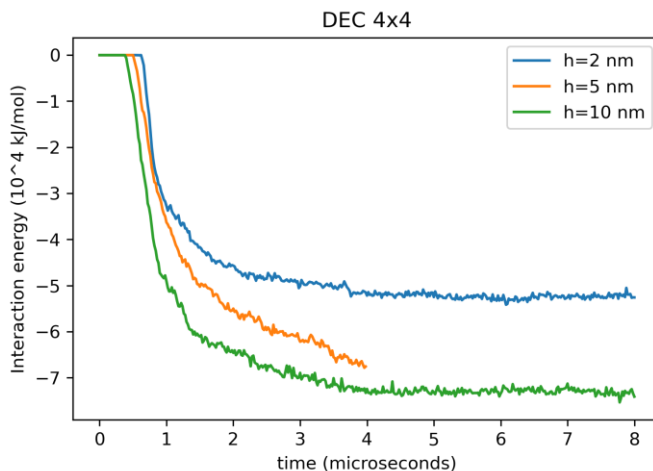


Figure 14: Evolution of interaction energy between a lipidic vesicle and a 4x4 SAM system with DEC coating. It is important to see how the energy is lower on this case compared to the previous one, which presented a smaller surface.

### 6.2.2. Observations.

As mentioned, the interaction of a vesicle with different modelled nanopillars is simulated. We observe that the surfaces with a greater nanopillar height achieve a lower state of energy as time advances in the simulation, due to the formation of stabler conformations. A similar behaviour is observed in both the simulations conducted with a surface of 3x3 and 4x4 nanopillars. As the height of the pillar increases from 2 to 10 nm, the system becomes more stable, with a lower interaction energy being calculated, although in the 3x3 case the difference is much less noticeable than in the 4x4 surface. To obtain the result, the interaction between the CHOL and POPC beads of the vesicle and the beads that describe the surface: SUP, SUPF and DEC has been studied. After an analysis with VMD, it is seen that the vesicle breaks and forms adducts with the surface, then giving a reason for the great decrease in energy during the simulation.

## 6.3 SURFACE FREE ENERGY DETERMINATION

The characterization of the surface is finished by performing an exhaust determination of its Surface free energy following Wu and OWRK model. This step will draw conclusions on the applications of the given surfaces, as determining the surface free energy of a material will retrieve

the effect of polar and disperse interactions on the properties of a material, more precisely in those related to wettability. Linked to more advanced research, the application of methods to determinate the SFE is used to optimize the coating of surfaces, so the contact angle of different surfaces and the effect provoked by a change of polarity can be known before any change is made.

Firstly, OWRK model will be applied. This method is the standard method used to calculate the SFE of a surface giving contact data information with several liquids. To do so, the SFE is divided into a polar part and a disperse part, as previously stated on theoretical background. After this, Wu's model will be applied, another method used to obtain information about the SFE of a material, but with notable changes on the mean used in comparison with the earlier method.

### 6.3.1 OWRK model

OWRK is based on Young's equation (Eq.2), expanding the equation to solve the variable  $\sigma_s$ . The numerical expression that results from this expansion, Eq.4, is generated building on Fowkes method, which states that interfacial tension must be calculated considering the surface tension of the liquid and the solid:  $\sigma_s$  and  $\sigma_l$ . Also, each tension is divided in polar and disperse parts and the interaction between the similar phases is considered. These phases are the polar and disperse parts, as stated on OWRK's subsection on theoretical background. Note that OWRK model is characteristic for employing the geometric mean of the interactions, as it can be seen on Eq.4.

When applying a SFE calculation method to a real case, Fowkes mentions that the determination must take place in two steps. First, the disperse part is calculated with a purely disperse liquid in this project hexadecane plays that role, and then polar components are calculated with the other solvents that contain a positive polar part, water, and ethanol.<sup>[10]</sup>

$$\sigma_s = \sigma_{ls} + \sigma_l \cdot \cos \theta \quad (2)$$

$$\sigma_{ls} = \sigma_l + \sigma_s - 2 (\sqrt{\sigma_s^D \sigma_l^D} + \sqrt{\sigma_s^P \sigma_l^P}) \quad (4)$$

$$\text{Combined: } 2 (\sqrt{\sigma_s^D \sigma_l^D} + \sqrt{\sigma_s^P \sigma_l^P}) = \sigma_l (1 + \cos \theta) \quad (8)$$



### 6.3.2 Wu's model

On the other hand, Wu's model is generated with a different mathematical approach. On this case, the harmonic mean of the interactions is used to generated Eq.4

$$\sigma_s = \sigma_{ls} + \sigma_l \cdot \cos \theta \quad (2)$$

$$\sigma_{ls} = \sigma_l + \sigma_s - 4 \left( \frac{\sigma_s^D \sigma_l^D}{\sigma_s^D + \sigma_l^D} + \frac{\sigma_s^P \sigma_l^P}{\sigma_s^P + \sigma_l^P} \right) \quad (5)$$

$$\text{Combined: } 4 \left( \frac{\sigma_s^D \sigma_l^D}{\sigma_s^D + \sigma_l^D} + \frac{\sigma_s^P \sigma_l^P}{\sigma_s^P + \sigma_l^P} \right) = \sigma_l (1 + \cos \theta) \quad (9)$$

It is important to note that using a harmonic mean gives more emphasis on the individual interactions, polar or disperse, in comparison with a geometric mean, so the results between both methods may differ.

### 6.3.3 Numerical determination

In our case, water, ethanol, and hexadecane have been used as solvents. The following table includes the breakdown of surface tension into polar and disperse parts:

	$\sigma_l$ [mJ/m <sup>2</sup> ]	$\sigma_l^d$ [mJ/m <sup>2</sup> ]	$\sigma_l^p$ [mJ/m <sup>2</sup> ]
Water	72.8	21.8	51.0
Hexadecane	27.6	27.6	0
Ethanol	23.2	21.2	2.0

Table.6: Breakdown of surface tension into polar and disperse parts for the solvents used on the simulations.

Data from the previous Table.4, based on the first contact angle determination method, in addition to the calculated contact angles of every solvent will form a system of equations that, once solved, will give us the value for  $\sigma_s$  in mJ/m<sup>2</sup>.

As an example, for 6x6 h2, the following equations can be obtained applying OWRK's model:

$$(1 - \text{Water}): 2(\sigma_s^D * 21.8)^{1/2} + 2(\sigma_s^P * 51.0)^{1/2} = 72.8 (1 + \cos 68)$$

$$(2 - \text{Ethanol}): 2(\sigma_s^D * 21.2)^{1/2} + 2(\sigma_s^P * 2.0)^{1/2} = 23.2 (1 + \cos 36)$$

$$(3 - \text{Hexadecane}): 2(\sigma_s^D * 27.6)^{1/2} + 2(\sigma_s^P * 0)^{1/2} = 27.6 (1 + \cos 25)$$

Solving the system resulting from equations (1) and (3) grants the following result:  $\sigma_s^D = 25.07$  mJ/m<sup>2</sup> and  $\sigma_s^P = 13.93$  mJ/m<sup>2</sup>.

On the other hand, applying Wu's model:

$$(1 - \text{Water}): 4 ((\sigma_s^D * 21.8 / \sigma_s^D + 21.8) + (\sigma_s^P * 50.8 / \sigma_s^P + 50.8)) = 72.8 (1 + \cos 68)$$

$$(2 - \text{Ethanol}): 4 ((\sigma_s^D * 21.2 / \sigma_s^D + 21.2) + (\sigma_s^P * 2.0 / \sigma_s^P + 2.0)) = 23.2 (1 + \cos 36)$$

$$(3 - \text{Hexadecane}): 4 ((\sigma_s^D * 27.6 / \sigma_s^D + 27.6) + (\sigma_s^P * 0 / \sigma_s^P + 0)) = 27.6 (1 + \cos 25)$$

Solving the system resulting from equations (1) and (3) grants the following result:  $\sigma_s^D = 25.63$  mJ/m<sup>2</sup> and  $\sigma_s^P = 25.04$  mJ/m<sup>2</sup>. As observed, each component has a higher value on Wu's model.

The solutions to every system are collected on the following tables, using only hexadecane and water as the input equations.

	6x6			8x8		
Nanopillar height (nm)	$\sigma_s^D$ [mJ/m <sup>2</sup> ]	$\sigma_s^P$ [mJ/m <sup>2</sup> ]	$\sigma_s$ [mJ/m <sup>2</sup> ]	$\sigma_s^D$ [mJ/m <sup>2</sup> ]	$\sigma_s^P$ [mJ/m <sup>2</sup> ]	$\sigma_s$ [mJ/m <sup>2</sup> ]
2	25.07	13.93	39.00	25.63	24.95	50.58
5	27.60	11.60	39.20	27.60	12.76	40.36
10	27.60	9.94	37.54	27.60	9.41	37.01

Table.7: SFE results applying OWRK's model and the contact angle from table.4.

	6x6			8x8		
Nanopillar height (nm)	$\sigma_s^D$ [mJ/m <sup>2</sup> ]	$\sigma_s^P$ [mJ/m <sup>2</sup> ]	$\sigma_s$ [mJ/m <sup>2</sup> ]	$\sigma_s^D$ [mJ/m <sup>2</sup> ]	$\sigma_s^P$ [mJ/m <sup>2</sup> ]	$\sigma_s$ [mJ/m <sup>2</sup> ]
2	25.13	18.01	43.14	25.66	27.50	53.16
5	27.60	16.11	43.71	27.60	18.22	45.82
10	27.6	14.58	42.18	27.60	14.08	41.68

Table.8: SFE results based on Wu's model and contact angle data from table.4.

As indicated previously, the main difference between the methods is the mathematical approach used to determine the results, so the importance of individual interactions is highlighted on Wu's model, hence the higher values for the polar component.

### 6.3.4 Observations

The result of the different calculations is comprised on the range  $\sigma_s = 37.01 \text{ mJ/m}^2$  to  $\sigma_s = 53.16 \text{ mJ/m}^2$ . This surface free energy range is typically present on polymers, such as carbon fibre, materials typically used due to their stability when in contact with other materials. Compared to other materials, like glass or metals, this surface presents the lower SFE value of them all, making them to form a smaller interface to minimize the higher state of energy when interacting with other materials and profit their wetting properties. The following table contains a brief collection of typical SFE values:

Material	Surface free energy [ $\text{mJ/m}^2$ ]
Glass	83.4 <sup>[19]</sup>
Copper	1650.0 <sup>[20]</sup>
PTFE	19.0 <sup>[21]</sup>

Table.9: SFE values for several materials.

Applying this to a real case, this DEC surface can be used as a modifier on antibacterial paints, the low SFE arises from the weak bonds between the particles, then the oleophilic properties of DEC will make the bacteria interact with the surface and their cellular membranes will break.

## 6.4 SIMULATION OF NEW SURFACES

It is possible to extend the systematic characterization of surfaces to any type of surface. This project starts with the modelling and characterization of a hydrophobic but oleophilic surface, feature that is achieved by coating the surface with DEC. To continue with this line, a D2F molecule is now used as the coating, molecule that will present oleophobic and hydrophobic properties. Both the DEC and D2F molecules are modelled as the following figure:

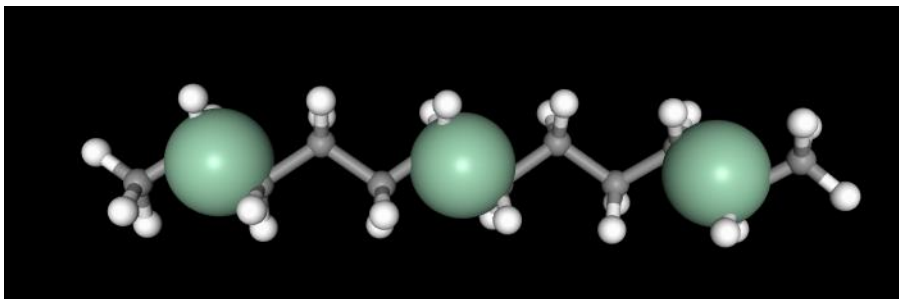


Figure 15: Coarse-grained model for DEC and D2F molecules, each green sphere represents a bead. For the DEC – dodecane molecule, each bead has the same characteristics as it is represented by beads  $C_1$ - $C_1$ - $C_1$ , while D2F- dodecane – 2 fluorinated is  $C_1$ -CX-CX, where CX are bigger beads in comparison with  $C_1$ , used to represent the fluorinated positions.

Previously, oleic solvents like hexadecane and ethanol, formed by an apolar or oleic part and a polar part, fully interacted with the surfaces presenting low contact angles and interaction energies. Now, this behaviour is expected to change, as the surface will be oleophobic. This can be extended to the interaction with the lipidic vesicle, as DEC – coated surfaces interacted strongly with them and deformed the vesicle, now the behaviour is expected to change, forming less interactions with a vesicle that will remain stable during the simulation, fact that is studied under this section.

#### 6.4.1 Interaction with Vesicles

As stated before, the new surface shouldn't interact strongly with lipid vesicles, thereby to know the mechanisms that the new surface undergoes when interacting with living cells, simulations between the SAMs and vesicles have been generated. These simulation follows the same structure compared to the DEC one: a SAM, formed with the previous surface and the new coating beads, has been placed in a simulation box that contains a lipid vesicle, modelled with POPC lipids and cholesterol molecules. The following results regarding the interaction energy can be extracted when the system has achieved equilibrium:

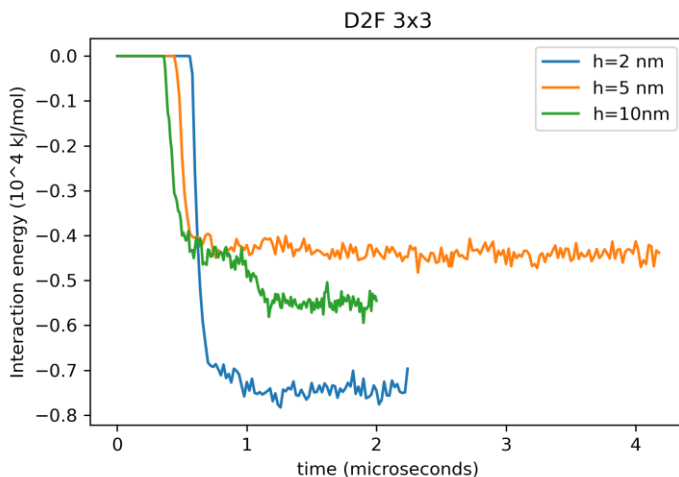


Figure 16: Evolution of interaction energy between a lipidic vesicle and a 3x3 SAM system with D2F coating. The modelled vesicle interacts with the D2F coating, with oleophobic characteristics, so the interaction energy doesn't acquire low values, as it is not stable.

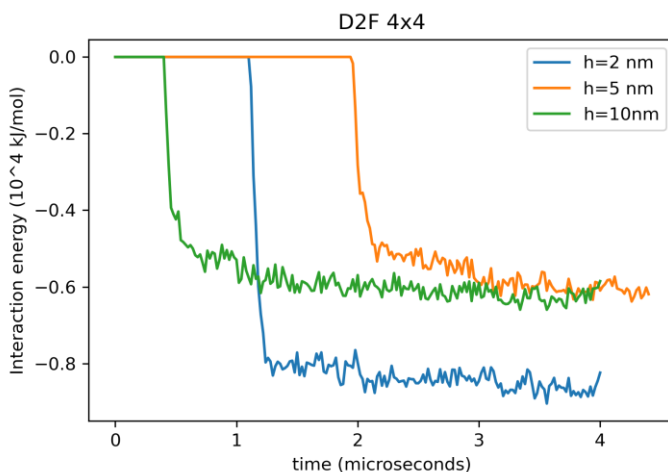


Figure 17: Evolution of interaction energy between a lipidic vesicle and a 4x4 SAM system with D2F coating. Compared to the previous case there is not much difference as the interaction energy lowers by less than  $1 \cdot 10^4$  kJ/mol in each system.

It can be seen how D2F systems achieve a less negative energy than the ones coated with DEC. This is due to the properties of D2F, as it is an oleophobic molecule that doesn't interact well with lipids like the ones conforming the modelled vesicle. It can be seen how the smaller systems, those of  $h = 2$  nm are the most stable due to a lesser quantity of unstable interactions. As the nanopillars are higher, the interaction energies are less negative, being the energies related to  $h = 5$  nm and  $h = 10$  nm almost equal.

This will result in the repulsion of the cells that encounter the coating, as the fluorinated surface, both hydrophobic and oleophobic, will repel any material, like the lipidic membranes that interact with the surface. In counterpart with the DEC coating, this new surface can't be employed on situations where bactericidal properties are desired, but it isn't suitable for cellular growth. The following figure shows the state of the lipidic membrane at the end of the equilibrium:

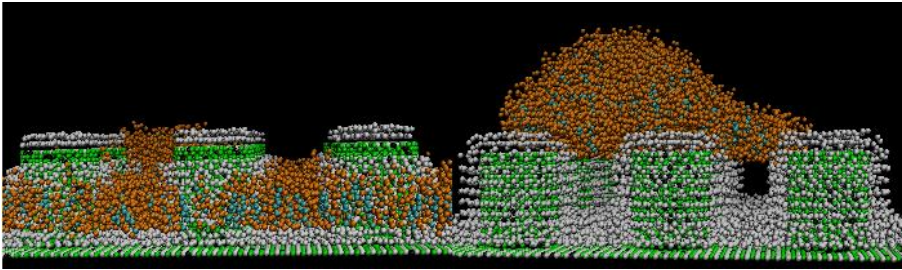


Figure 18: Comparison of the state of the cellular membrane at the end of the simulation. Regarding the surface, SUP beads are green, SUPF beads black and coating beads are white. Lipid vesicle beads have been represented as orange beads for POPC and cyan beads for CHOL. It is seen in the left part how DEC coating breaks the lipid vesicle, meanwhile D2F does not interact strongly with the lipidic components, only causing an opening in the base of the lipidic membrane, resulting in the conformation that is seen on the right. Via VMD.

## 7. CONCLUSIONS

After all the data has been analysed, the following conclusions have been recapped:

As the area of contact between the surface coated with the oleophilic DEC and the dispersive solvent increased, a more stable system was found at the equilibrium. On the other hand, polar solvents followed the contrary tendency due to the hydrophobic properties of the surface. The contact angle has been found higher on completely polar solvents, meanwhile a lower contact angle, or even total wetting on solvents that presented a dispersive behaviour. This fact originated a low disperse SFE, making the surface a good substrate to interact with other oleic molecules.

The energies were way higher on systems with a D2F coating, as they were both hydrophobic and oleophobic, not allowing the formation of more favourable situations that stabilised the system.

The DEC coating caused the lipidic vesicles to break, as they were able to interact with the oleic parts of the vesicle. The larger the area of the surfaces, the greater the effect. On the contrary case, systems with D2F coating didn't interact strongly with the vesicle, resulting in the settling of the lipid vesicle above the nanopillars, opening their base and generating high energy systems.

The simulations have shown that a DEC coating is suitable for bactericidal surfaces. Applications such as its employment on hospital walls are possible, meanwhile the D2F surface doesn't present these properties.

In conclusion, the surfaces with a DEC coating are featured by a low polar SFE value, making them extraordinary bad to interact with different objects with polar characteristics, but their oleophilic properties can help them interact with certain materials. More precisely, they excel when interacting with oleic particles, thanks to the oleophilic nature of the DEC molecule. On the other hand, surfaces coated with D2F don't interact with oleic particles due to the oleophobic nature of the particle. This project includes a brief characterization of the D2F surface, as only their interaction with lipidic vesicles is studied.





## 8. REFERENCES AND NOTES

1. Dobrzanski, Leszek. Significance of materials science for the future development of societies. *Journal of Materials Processing Technology*. **2006**, 175, 133-148.
2. Thornton, K., Qi, L., Uberuaga, B.P. et al. Recent advances and future needs in computational approaches for materials discovery and development. *MRS Communications*. **2022**, 12, 989–990.
3. Amy Y. Shih, Anton Arkhipov, Peter L. Freddolino, and Klaus Schulten. Coarse grained protein-lipid model with application to lipoprotein particles. *Journal of Physical Chemistry B*. **2006**, 110, 3674-3684.
4. I. Junkar, Chapter Two - Interaction of Cells and Platelets with Biomaterial Surfaces Treated with Gaseous Plasma. *Advances in Biomembranes and Lipid Self-Assembly*. **2016**, volume 23, pages 25-39.
5. Marrink, Siewert, J. et al. The MARTINI force field: Coarse grained model for biomolecular simulations. *Journal of physical chemistry B*. **2007**, 111 (27), 7812- 7824.
6. Su J, Charmchi M, Sun H. A Study of Drop-Microstructured Surface Interactions during Dropwise Condensation with Quartz Crystal Microbalance. *Scientific Reports*. **2016**, 6, 35132.
7. Koishi, Takahiro; Yasuoka, Kenji; Fujikawa, Shigenori; Ebisuzaki, Toshikazu; Chen, Xiaohong. Coexistence and transition between Cassie and Wenzel state on pillared hydrophobic surface. *Proceedings of the National Academy of Sciences of the United States of America*. **2009**, 106. 8435-40
8. Daiki Murakami, Hiroshi Jinnai, and Atsushi Takahara. Wetting Transition from the Cassie–Baxter State to the Wenzel State on Textured Polymer Surfaces. *Langmuir*. **2014**, 30 (8), 2061-2067
9. Yuan, Y., Lee, T.R. (2013). Contact Angle and Wetting Properties. *Surface Science Techniques*. **2013**, 51, 3-34.
10. F. M. Fowkes. Attractive Forces at Interfaces. *Industrial and Engineering Chemistry*. **1964**, 56, 12, 40-52.
11. A. Kozbial, Z. Li, et al. Study on the surface energy of graphene by contact angle measurements. *Langmuir*. **2014**, 30, 8598-8606.
12. Kaelble, H. Dispersion-Polar Surface Tension Properties of Organic Solids. *J. Adhesion*. **1970**, 2, 66-81.
13. Owens, D.; Wendt, R. Estimation of the Surface Free Energy of Polymers. *J. Appl. Polym. Sci*. **1969**, 13, 1741-1747
14. Guo, L., Wong, P. & Guo, F. Identifying the optimal interfacial parameter correlated with hydrodynamic lubrication. *Friction*. **2016**, 4, 347–358.
15. Zdziennicka, A., Krawczyk, J., Szymczyk, K., & Jańczuk, B. Components and parameters of liquids and some polymers surface tension at different temperature. *Colloids and Surfaces A: Physicochemical and Engineering Aspects*. **2017**, 529, 864–875
16. Gurau, Vladimir & Bluemle, Michael & Castro, Emory & Tsou, Yu-Min & Mann, J. & Zawodzinski, Thomas. Characterization of transport properties in gas diffusion layers for proton exchange membrane fuel cells: 1. Wettability (internal contact angle to water and surface energy of GDL fibers). *Journal of Power Sources*. **2006**, 160. 1156-1162.
17. M. Palencia. Surface free energy of solids by contact angle measurements. *J. Science with Technological Applications*. **2017**, 2, 84-93

18. Rafaël Sibilo, Ilaria Mannelli, Ramon Reigada, Carlo Manzo, Mehmet A. Noyan, Prantik Mazumder, and Valerio Pruneri. Direct and Fast Assessment of Antimicrobial Surface Activity Using Molecular Dynamics Simulation and Time-Lapse Imaging. *Analytical Chemistry*. **2020**, 92 (10), 6795-6800.
19. Rhee, S.-K. Surface energies of silicate glasses calculated from their wettability data. *Journal of Materials Science*. **1977**, 12 (4): 823–824.
20. Udin, H. Grain Boundary Effect in Surface Tension Measurement. *JOM*. **1951**, 3, 63.
21. Kinloch, A. J. et al. Adhesion & Adhesives: Science & Technology. *British Polymer Journal*. **1987**, 20, 300-300

## 9. ACRONYMS

**SFE:** Surface Free energy

**CG:** Coarse-Grained

**SAM:** Self-assembled monolayer

**MD:** Molecular dynamics

**DEC:** Dodecane

**D2F:** Dodecane 2-Fluorinated

**OWRK:** Owens-Wendt-Rabel-Kaelble

**LJ:** Lennard-Jones

**(CB):** Cassie-Baxter

**(W):** Wenzel

**POPC:** 1-Palmitoyl-2-oleoyl-sn-glycero-3-phosphocholine

**CHOL:** Cholesterol



# APPENDICES



# APPENDIX 1: GROMACS INPUT FILES

.gro input file must contain information about which bead represents a determined molecule and their coordinates, wrote as:

Line 1: Title

Line 2: Total bead number

Line 3 onwards: molecule            bead    bead number    x        y        z

Last line: box length: xbox        ybox    zbox

.itp input file must contain a description of the different molecules conforming the system, with the following structure:

;;; Molecule name

[moleculetype]

; molname    nrexcl

Name        1

[atoms]

; id   type    resnr    residu   atom    cgnr    charge

1   BEAD   1        Name   BEAD   1        0

If the molecule is represented with multiple beads, information regarding the bonds must be included:

[bonds]

; i j    funct    length    force.c.

id's 1=bond    Amstrongs    k

[angles]

; i j k                    funct    angle    force.c.

(id of the bead)        2=angle    degrees    k

.ndx input file: It must define the different atom groups present in the simulated system. Its structure is wrote as:

```
[System]
```

```
# index number of all atoms
```

```
[Other]
```

```
# index number of all atoms
```

```
[Group 1]
```

```
# index number of atoms included in group 1
```

```
[Group 2]
```

```
# index number of atoms included in group 2
```

```
[Group N]
```

```
# index number of atoms included in group N.
```

```
[arrel]
```

```
# index of all atoms
```

- .mdp input file: This file must contain the instructions for the simulation. In the section "integrator" we must specify integrator = md for molecular dynamics simulations. The option integrator = steep would give instructions to begin an energy minimisation on the system.

-.top input file: It must contain the total number of molecules in the system and their definition, defined previously in a .itp file. It's structure is:

```
#include " archives.itp"
```

```
[system]
```

```
System name
```

```
[molecules]
```

```
Group1 #number of molecules
```

```
GroupN #number of molecules
```



## APPENDIX 2: FORTRAN PROGRAMS – SAM GENERATION

A Fortran program is used to generate SUP, SUPF, Coating and solvent atoms at random locations. The code generates a random coordinate, as can be seen on the following lines, applied to SUP beads:

```
implicit real*8(a-h,o-z)
open(unit=8,file='support_surface.gro')
NP=3
r=2.
h=10.
xbox=25.
ybox=25.
xsep=0.5
pi=acos(-1.0)
nx=(xbox/xsep)
ny=(ybox/xsep)
sp=xbox/float(NP)
imol=1
iat=1
do ix=1,nx
  do iy=1,ny
    x=(float(ix-1)*xbox/float(nx))
    y=(float(iy-1)*ybox/float(ny))
    iflag=0
    do i=1,NP
      do j=1,NP
        xcenter=(sp/2.)+float(i-1)*sp
        ycenter=(sp/2.)+float(j-1)*sp
        dist=((xcenter-x)*(xcenter-x))+((ycenter-y)*(ycenter-y))
```

```

                                dist=sqrt(dist)
                                if (dist.le.r) iflag=1
                                enddo
                                enddo
                                if (iflag.eq.1) then
                                    z=h
                                else
                                    z=0.
                                endif
                                write(8,115)imol,iat,x,y,z
                                imol=imol+1
                                iat=iat+1
                                if ((iy.lt.ny).and.(ix.lt.nx)) then
                                    x=x+(xsep/2.)
                                    y=y+(xsep/2.)
                                    iflag=0
                                    do i=1,NP
                                        do j=1,NP
                                            xcenter=(sp/2.)+float(i-1)*sp
                                            ycenter=(sp/2.)+float(j-1)*sp
                                            dist=((xcenter-x)*(xcenter-
x))+((ycenter-y)*(ycenter-y))
                                            dist=sqrt(dist)
                                            if (dist.le.r) iflag=1
                                        enddo
                                    enddo
                                if (iflag.eq.1) then
                                    z=h

```

```

else
    z=0.
endif
write(8,115)imol,iat,x,y,z
imol=imol+1
iat=iat+1
endif
enddo
enddo
do i=1,NP
    do j=1,NP
        xcenter=(sp/2.)+float(i-1)*sp
        ycenter=(sp/2.)+float(j-1)*sp
        nz=1+(h/xsep)
        xnfi=2.*pi*r/xsep
        nfi=xnfi+1
        do iz=1,nz+1
            do ifi=1,nfi+1
                fi=float(ifi-1)*2.*pi/float(nfi)
                z=(float(iz-1)*h/float(nz))
                x=xcenter+r*cos(fi)
                y=ycenter+r*sin(fi)
                write(8,115)imol,iat,x,y,z
                imol=imol+1
                iat=iat+1
                if (iz.le.nz) then
                    z=z+(xsep/2.)
                    fi=fi+(pi/float(nfi))
                endif
            enddo
        enddo
    enddo
enddo

```

```
x=xcenter+r*cos(fi)
y=ycenter+r*sin(fi)
write(8,115)imol,iat,x,y,z
imol=imol+1
iat=iat+1
endif
enddo
enddo
enddo
write(8,*)xbox,xbox,2.*h
115 format(I5,'SUP NaN',I5,3(1X,F7.3))
9 format(A20,3(1X,F7.3),3(1X,F7.4))
10 format(A80)
11 format(I5)
end
```

## APPENDIX 3: PYTHON PROGRAMS – DATA ANALYSIS

A Python script is implemented to perform data analysis. We open the data file .xvg and select a certain data column, as can be seen on the attached document:

```
import pandas as pd
import matplotlib.pyplot as plt
import numpy as np
import sys

data = pd.read_csv('6x6output_h2_w_1.xvg', skiprows=34, engine='python', sep='\\s+',
header=None)

dataXsimulacion = data.iloc[:,0]
dataXREAL= dataXsimulacion * 4
ArrayX= np.array(dataXREAL)
X= ArrayX/10**6
dataY1= data.iloc[:,4]
dataY2= data.iloc[:,5]
dataY3= data.iloc[:,8]
dataY4= data.iloc[:,9]
dataY5= data.iloc[:,11]
dataY6= data.iloc[:,12]

dataRECVES = dataY2 + dataY4 + dataY5 + dataY6
Array= np.array(dataRECVES)
Y= Array/(10**4)

plt.plot(X, Y)
plt.xlabel("tiempo (microsegundos)")
plt.ylabel("Energía de interacción (10^4 kJ/mol)")
plt.savefig("6x6output_h2_w_1.png", format= "png", dpi=300)

plt.show()
```